Catalysis Today 178 (2011) 181–186

Contents lists available at ScienceDirect

Catalysis Today

journal homepage: www.elsevier.com/locate/cattod

The selective hydrogenation of acetylene in the presence of carbon monoxide over Ni and Ni–Zn supported on $MgAl_2O_4$

David L. Trimm[a], Noel W. Cant[b,*], Irene O.Y. Liu[c]

[a] CSIRO Earth Science and Resource Engineering, Clayton South, VIC 3169, Australia
[b] Department of Chemistry and Biomolecular Sciences, Macquarie University, NSW 2109, Australia
[c] School of Chemical Sciences and Engineering, The University of New South Wales, NSW 2053, Australia

ARTICLE INFO

Article history:
Available online 29 July 2011

Keywords:
Acetylene hydrogenation
Nickel–zinc catalyst
Carbon monoxide inhibition
Selectivity

ABSTRACT

The effect of gaseous carbon monoxide on the hydrogenation of acetylene over Ni supported on $MgAl_2O_4$ in the presence and absence of zinc dopants has been investigated. Both carbon monoxide and zinc inhibit activity to a considerable extent. Carbon monoxide also lowers the selectivity to ethane substantially. Zinc causes some reduction in selectivity in the absence of carbon monoxide but only at very high conversions when it is present.

© 2011 Elsevier B.V. All rights reserved.

1. Introduction

Production of ethylene by the steam cracking of ethane is inevitably accompanied by the formation of acetylene at concentrations much higher than the low ppmv level that can be tolerated by the catalysts currently used for polyethylene manufacture. The standard method for acetylene removal is selective catalytic hydrogenation, ideally to ethylene alone, which can be carried out either in excess hydrogen (front-end) or with close to stoichiometric quantities of hydrogen (tail-end). Palladium-based catalysts, moderated by the inclusion of silver [1–3], and/or by the inclusion of carbon monoxide (denoted CO from now on) in the feed, are now the preferred choice [4–6]. Nickel catalysts have been used in the past, especially in front-end applications [7,8].

Recent DFT calculations have predicted that Ni–Zn alloys should exhibit selectivities similar to that of Pd–Ag systems and hence prove more cost-effective given the large difference in metal price [9]. The authors tested the prediction for metals supported on a $MgAl_2O_4$ spinel using a model feed containing ~0.07% C_2H_2, 1.33% C_2H_4 and 0.67% H_2. A $NiZn_2$ alloy proved more selective than Pd alone at high acetylene conversions and likewise $NiZn_3$ was more selective than $PdAg_3$ [9].

In principle, improvements in the selectivity to ethylene can arise either at the primary stage, the hydrogenation of acetylene to ethylene,

$$C_2H_2 + H_2 \rightarrow C_2H_4 \quad (1)$$

versus the parallel conversion to undesired ethane,

$$C_2H_2 + H_2 \rightarrow C_2H_6 \quad (2)$$

or at the secondary stage, the undesired hydrogenation of ethylene to ethane

$$C_2H_4 + H_2 \rightarrow C_2H_6. \quad (3)$$

Moderators can influence both stages with CO thought to restrict reaction (3) through the inhibition of ethylene adsorption.

In recent work we have examined this question for a 2% Ni/SiO_2 catalyst with and without CO included in the feed [10]. CO was found to both reduce the extent to which ethane was formed when acetylene was being hydrogenated at conversions up to 90% and to inhibit the further reaction of ethylene, both derived from acetylene or added to the feed, at higher conversions. The aim of the present work was to extend the comparison to a nickel–zinc system. The experiments have been carried out without ethylene in the feed, which limits the industrial relevance, but enables a more accurate assessment of the relative effects of CO and Zn on the extent of reaction (1) versus (2), and at high conversions, of reaction (3) as well.

The initial intention was to study nickel–zinc alloys supported on silica gel but it proved difficult to prepare such systems with an exact alloy composition. Zinc salts reacted with silica during impregnation, drying and calcination to form amorphous zinc silicates [11,12]. XRD measurements of the preparations after reduction gave a lattice parameter for alloy component that was larger than that expected for nickel alone, but corresponded to a zinc content well below that expected from the Ni–Zn ratio in the impregnating solutions. Following Studt et al. [9], a $MgAl_2O_4$ spinel

* Corresponding author. Tel.: +61 2 9850 8285; fax: +61 2 9850 8313..
E-mail address: noel.cant@mq.edu.au (N.W. Cant).

0920-5861/$ – see front matter © 2011 Elsevier B.V. All rights reserved.
doi:10.1016/j.cattod.2011.06.025

was used instead. The $MgAl_2O_4$ support available to us had a surface area approximately one-fifth of theirs and, in consequence, the total metal content of our preparations was set at ~2 wt% rather than the 10 wt% used in their work.

2. Experimental

The two catalysts studied here were prepared in a manner similar to that described by Studt et al. [9] except for the lower metal content. A commercial $MgAl_2O_4$ support (Haldor Topsoe A/S, surface area 12 m^2/g, mean pore diameter ~15 nm) was impregnated with aqueous nitrate solutions to give nominal loadings of 2.0 wt% Ni (for the catalyst referred to as Ni-only from now on), 0.7 wt% Ni/1.5 wt% Zn (referred to as $NiZn_2$) and 1.5 wt% Zn (a comparison Zn-only preparation). The bulk preparations were calcined in air in a static oven for 3–4 h at 450 °C. Test samples (0.2 g) were reduced in the reactor in pure H_2 on a temperature ramp (3 °C/min) that concluded with 5 h at 400 °C and then cooled to the starting reaction temperature in pure H_2 overnight. The standard feed comprised 2% C_2H_4, 20% H_2, 0 or 550 ppmv (0.055%) CO in a helium carrier at a total flow rate of 50 cm^3/min.

The test system was a simplified version of that described in detail previously [10]. It comprised a 6 mm I.D. Pyrex reactor arranged vertically with analysis of the exit gas every 10 min but with only one of the two chromatographs used previously in place. The single chromatograph (an MTI 200) was fitted with two columns, a molecular sieve 5A one (which enabled analysis of firstly isobutene plus isobutane as a composite peak followed by CH_4 and CO and a Poraplot U one (for C_2H_4, C_2H_6, C_2H_2 and $C_3H_6 + C_3H_8$ as a composite). Unlike previously, analysis for n-C_4 and higher hydrocarbons was not possible but the total amount formed, including that deposited as carbonaceous matter on the catalyst, could be estimated with reasonable accuracy by mole balance calculations.

Powder XRD patterns were obtained using a Philips X'pert Pro MPD diffractometer operating with a Cu Kα source, a step size of 0.013° (2θ basis) and a scan rate of 5°/min. The metal surface area was estimated by the pulse chemisorption of CO at room temperature using a Micromeritics Autochem 2950 analyser. Large samples of catalyst (~0.75 g) were reduced as above, cooled in helium and then exposed to pulses of 10% CO in helium delivered at intervals of 3–10 min from a loop with volume of ~0.4 mL. The sample saturated after 2–8 pulses with only small amounts of physically adsorbed material, swept off between pulses, adsorbed subsequently. Temperature programmed reduction (TPR) was conducted on a similar Micromeritics Autochem 2920 instrument with a liquid nitrogen trap for water removal ahead of the thermal conductivity detector. Samples of the calcined starting materials weighing ~0.2 g were ramped at 10 °C/min in 10% H_2/Ar flowing at 50 cm^3(STP)/min.

3. Results and discussion

3.1. Reduction and characterisation

The pretreatment procedure used here (calcination in air at 450 °C followed by reduction concluding at 400 °C) was chosen so as to match that used in the previous study of the Ni–Zn/$MgAl_2O_4$ system [9] with one exception, the use of 100% H_2 during reduction rather than the 10% H_2 in reference [9]. Regardless of the feed, the reduction of bulk NiO is thermodynamically favourable, with a K of ~350 at 400 °C for the reduction

$$NiO(s) + H_2(g) \leftrightarrow Ni(s) + H_2O(g) \quad K_{NiO} = P_{H_2O}/P_{H_2}.$$

The corresponding reduction of solid ZnO is unfavourable ($K_{ZnO} \approx 2 \times 10^{-6}$). However, the thermodynamic driving force for alloy formation renders the reduction of ZnO somewhat more favourable in combinations of NiO and ZnO. Calculations using data in Nash and Pan [13] for Ni–Zn alloys, and that in Barin [14] for the pure metals and oxides, indicated a K of ~0.04 for hydrogen reduction of a 1:2 NiO/ZnO mixture to an alloy. Thus reduction would be thermodynamically restricted. Nevertheless, if the reaction was not kinetically limited, a calculated reaction time of ~8 min would be sufficient for complete reduction of both NiO and ZnO in a 1:2 mixture of the two at 400 °C with the combination of metal oxide mass and hydrogen flow rate used here. According to the phase diagram [13], the final product would be a mixture of the β_1-NiZn and γ-$NiZn_3$ phases.

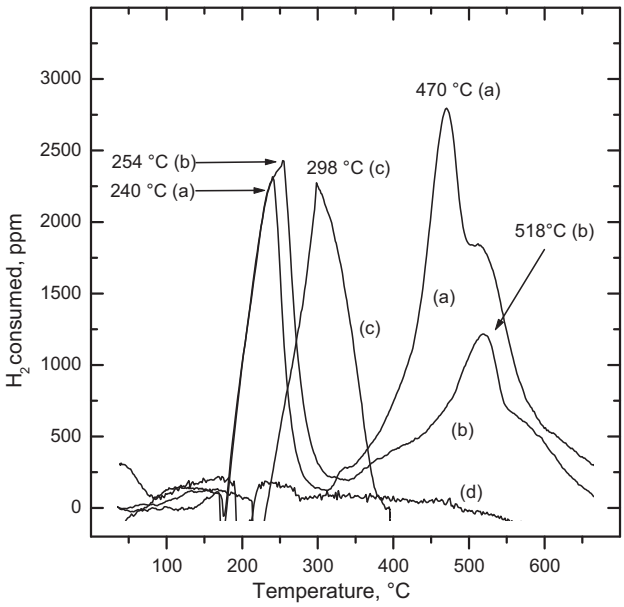

Fig. 1. Temperature programmed reduction of 0.2 g samples in 10% H_2/Ar with flow rate of 50 cm^3/min and ramp rate of 10 °C/min: (a) Ni/$MgAl_2O_4$ to 700 °C; (b) $NiZn_2$/$MgAl_2O_4$ to 700 °C; (c) 1.5 wt% Zn/$MgAl_2O_4$ to 400 °C then held for 1 h; (d) Zn/$MgAl_2O_4$ sample from (c) after reoxidation in 1% O_2/He for 1 h at 400 °C. The small regions with negative signals near 200 °C in some plots are due to flow rate changes when the liquid nitrogen trap for water removal was topped up.

Temperature programmed reduction of the three preparations in 10% H_2/Ar gave the results shown in Fig. 1. The trace for the nickel-only preparation (a) showed two peaks with the area of higher temperature one corresponding to a H_2/Ni ratio near unity, as expected for the reduction of NiO to Ni. The peak temperature (470 °C) was in reasonable agreement with the value of 420 °C reported by Gao et al. [15] for TPR of NiO/$MgAl_2O_4$ calcined briefly at 460 °C. It is likely that the lower temperature peak (at 240 °C) arose from the reduction of residual nickel nitrate, not fully decomposed during calcination, to nickel oxide as reported by Sietsma et al. [16]. In their work, a nickel nitrate on SBA-15 preparation decomposed in 5% H_2/Ar to yield NiO over the temperature range 220–310 °C, with reduction to the metal setting in at higher temperature. The stoichiometry of the initial reduction in NiO was not established but the products were shown to include NO (requiring a $H_2/Ni(NO_3)_2$ ratio of 3), N_2O (ratio 5) and NH_3 (ratio 8) but not NO_2 or O_2. On this basis residual $Ni(NO_3)_2$ equivalent to 6 to 20% of that initially deposited would be sufficient to account for the H_2 consumed during the low temperature peak.

The TPR results for the Zn-only sample, as carried out in two stages, conform to this picture. The first TPR, to 400 °C and then held, showed a single peak with a maximum at 298 °C (Fig. 1c). A second TPR (d) taken to much higher temperature after exposure of the sample from (c) to oxygen at 400 °C and cooling to room temperature, showed no definite reduction peak. This is as expected

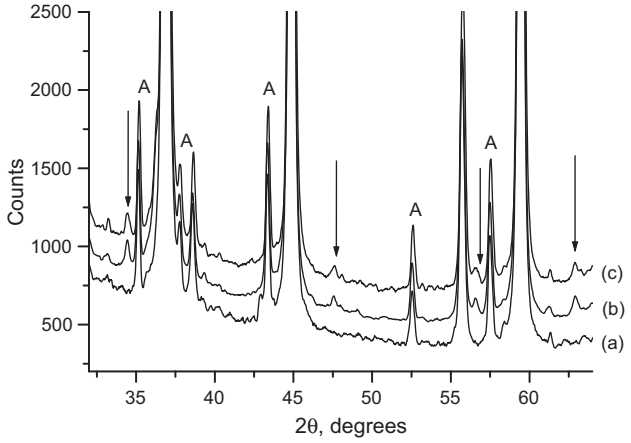

Fig. 2. Powder XRD patterns of (a) $MgAl_2O_4$ support; (b) calcined $NiZn_2/MgAl_2O_4$ preparation; (c) reduced $NiZn_2/MgAl_2O_4$ catalyst. Peaks denoted as A are due to α-Al_2O_3 present as an impurity in the support. The arrows point to the small peaks attributable to the zincite form of ZnO (JCPDS-IUDD pattern 01-079-0206). The patterns have been scaled so that the peaks of $MgAl_2O_4$ and α-Al_2O_3 at 2θ of 36.853° and 35.151° respectively had similar intensities (~30,000 and ~2000 counts, respectively) with plots (b) and (c) then offset upwards by 200 and 400 counts respectively.

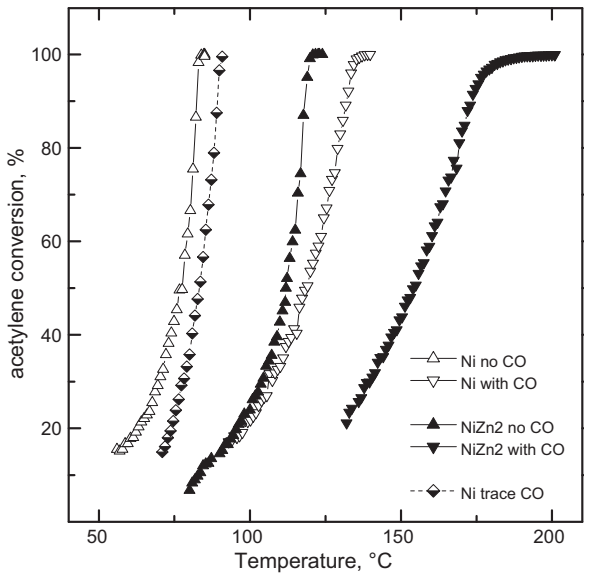

Fig. 3. Acetylene conversion versus temperature for $Ni/MgAl_2O_4$ and $NiZn_2/MgAl_2O_4$ catalysts under standard conditions with and without 550 ppmv CO present (0.2 g sample, 2% C_2H_2, 20% H_2 in He with total flow rate of 50 cm^3/min).

if the initial decomposition in hydrogen proceeded only as far as ZnO, which was not reduced subsequently due to the unfavourable thermodynamics noted above.

On this basis the two peaks seen during reduction of the $NiZn_2$ sample, (b) in Fig. 1, can be assigned as follows. The one at 254 °C arose from the reductive decomposition of residual nickel and zinc nitrates to their oxides. The second rather broad peak at 518 °C corresponded to the formation of the metals and/or alloys. The area of this peak, equivalent to a H_2/(Ni + Zn) ratio of 0.5–0.6, was greater than the Ni/(Ni + Zn) ratio of 0.33. Hence some of the zinc, of the order of one-quarter, was reduced. The reduction procedure prior to the catalytic measurements was somewhat different from the TPR ones. It used 100% H_2 rather than 10%, the ramp rate was slower and followed by hold period of 5 h, but the hold temperature of 400 °C was below the 518 °C of the second peak in Fig. 1. While some reduction of zinc appeared possible, there could be no certainty that any had taken place.

Powder XRD measurements (Fig. 2) were in general support of the above conclusions. The dominant phase in the pattern of the spinel support, responsible for all the off-scale peaks in Fig. 2(a), was cubic $MgAl_2O_4$ (JCPDS-ICDD pattern 01-074-1132). A small amount (~6%) of α-Al_2O_3 (pattern 00-43-1484) was present as an impurity. Diffractograms of the calcined and reduced Ni/spinel (not shown) exhibited no additional reflections attributable to NiO and/or Ni phases. Likewise, the patterns of the calcined and reduced $NiZn_2$/spinel, Fig. 2(b) and (c) respectively, showed no peaks attributable to nickel-containing phase or to any NiZn alloy. However small peaks due to ZnO (zincite, pattern 01-079-0206) at 2θ = 34.42° (the 0 0 2 reflections), 47.54° (1 0 2), 56.59° (1 1 0) and 62.86° (1 0 3) were evident in both. Their peak areas relative to those of $MgAl_2O_4$ and Al_2O_3 were not significantly different for the two materials, consistent with minor, if any, reduction of the zinc component. XRD measurements on used $NiZn_2/MgAl_2O_4$ catalysts showed the same ZnO peaks with similar intensities relative to support peaks.

The ZnO particles responsible for the peaks in Fig. 2(b) and (c) were quite large with an average crystallite size of ~35 nm (as calculated from line widths using the Scherrer equation). The XRD results for the reduced sample cannot preclude the formation of small amounts of phases containing Zn^0. While there are no documented examples of the formation of a NiZn alloy by the low temperature reduction of supported nickel oxide/zinc oxide mixtures it has been reported for unsupported mixed oxides made in particular ways [17]. Alloy formation is also well known for other zinc-containing catalysts, most notably the palladium–zinc system for the steam reforming of methanol where the effect on product distribution is dramatic [18].

The reduced form of both preparations did chemisorb small amounts of CO. Assuming the CO adsorbed on surface Ni atoms alone, with a CO/Ni_s ratio of unity and an area of 6.6×10^{-20} m^2/surface nickel atom [19], then the metal surface areas were 0.33 $m_{Ni}{}^2/g_{catalyst}$ for $Ni/MgAl_2O_4$ and 0.033 $m_{Ni}{}^2/g_{catalyst}$ for $NiZn_2/MgAl_2O_4$ with the latter value highly uncertain.

3.2. The effect of carbon monoxide on activity

The Ni/SiO_2 catalysts studied previously [10] showed substantial conversion when first exposed to a reaction mixture at temperatures of 50–100 °C. This was followed by a sharp drop in activity and then slow continuous deactivation [10]. The behaviour of the two $MgAl_2O_4$-based catalysts employed here was quite different. Their initial activity in the absence of CO was nearly zero at 100 °C but when the temperature was increased to above 130 °C the activity rose slowly to near complete conversion. The state of higher activity was retained when the catalyst was subsequently cooled to below 100 °C and through subsequent experiments if the catalyst samples were flushed with H_2 alone overnight. Long-term stability was not investigated. Repeated temperature ramp experiments (each taking ~2 h) showed a loss in activity of ~5% per run and this small loss was not noticeably different for Ni versus $NiZn_2$ catalysts nor for experiments with and without CO present.

Fig. 3 compares the behaviour of the Ni-only and $NiZn_2$ catalysts in their activated states in the absence and presence of 550 ppmv CO in terms of acetylene conversion when subjected to a slow temperature ramp (0.3 °C/min). It is apparent that CO lowers activity to considerable extent with temperatures approximately 40 °C higher required to achieve the same conversion with both catalysts. When compared with same quantity of CO present, the $NiZn_2$ samples are considerably less active than their Ni-only counterparts.

Table 1 shows apparent activation energies (E_a) calculated from Arrhenius plots for rates calculated from the conversions shown in Fig. 3 on the basis of the differential reactor approximation. This is

Table 1
Activities of $Ni/MgAl_2O_4$ and $NiZn_2/MgAl_2O_4$ catalysts at 100 °C.[a]

	CO (ppmv)	E_a (kJ/mol)	Rate (mmol g_{cat}^{-1} min^{-1})	Rate (mmol g_{Ni}^{-1} min^{-1})	Turnover frequency (s^{-1})
$Ni/MgAl_2O_4$	0	65	0.40	20	0.79
	Trace	101[b]	0.20	10	0.40[c]
	550	53	0.049	2.4	0.10
$NiZn_2/MgAl_2O_4$	0	63	0.054	8	1.1
	550	52	0.014	1.9	0.3

[a] For standard feed (2% C_2H_2 and 20% H_2) with extrapolation to 100 °C using the apparent activation energies shown.
[b] This value was artificially high because the trace quantities of residual CO were slowly flushed out of the system during the course of the temperature ramp, thus increasing activity.
[c] This activity was calculated assuming an apparent activation energy of 59 kJ/mol, the average of the uninhibited and CO-inhibited values.

reasonable assumption given that, on the basis of measurements with a Ni/SiO_2 catalyst [10], the reaction is likely to be close to zero order in acetylene (and that is the limiting reagent under the conditions used here). The values for E_a are slightly lower for the CO inhibited reaction than for the uninhibited one.

The activities, in terms of weight and apparent turnover frequency, shown in Table 1 were each calculated by extrapolation from the temperature giving 25% conversion in Fig. 3 to 100 °C using the experimental apparent activation energies. Irrespective of the units, inhibition by CO was a factor of ~8 for the Ni-only catalyst and ~4 for the $NiZn_2$ one. On a total weight of catalyst basis, the activity of $NiZn_2$ was lower than that of Ni-only by a factor of ~7 in the absence of CO and by a factor of ~4 when CO was present. However, the difference between $NiZn_2$ and Ni-only was reduced to a factor of approximately two when activity was expressed in terms of the weight of Ni due to the three-fold lower Ni content of the $NiZn_2$ sample. In terms of apparent turnover frequency, the $NiZn_2$ sample even appeared more active than Ni-only sample but the imprecision in the determination of the surface area of the nickel in the $NiZn_2$ sample is such that this difference may not be real.

The run denoted "Ni trace CO" in Fig. 3 was carried out using a Ni-only catalyst and a nominally CO-free feed but immediately after an experiment using a CO-containing feed over the same sample. The activity during this "Ni trace CO" experiment was significantly less relative to that when the CO was absent (the plot denoted "Ni no CO"), particularly in the initial stages of the ramp. Residual CO in the system, either in the gas phase at concentrations below the detection limit of the gas chromatograph (~30 ppmv), or retained on the nickel surface, is the likely cause of the lower activity. Flushing of CO from the system as the temperature ramp proceeded, with acceleration in activity, is the likely explanation for the much higher value for E_a evident for the run in Table 1.

3.3. The effect of carbon monoxide and zinc on ethane production

Fig. 4 compares the systems in terms of the performance parameter used by Studt et al. [9], the relationship between ethane production and acetylene conversion. The plots are linear to at least 70% conversion and then rise steeply. The implication is that the primary selectivity, i.e. reaction (2) versus (1), is constant over an extended range of conversions and, correspondingly, over a considerable spread of temperatures (~30 °C for conversions from 10 to 70%). Thus, although the selectivities of the catalysts are being compared at different temperatures, this factor is unlikely to be the major cause for the selectivity difference. It is apparent that CO lowered ethane production substantially for both catalysts and also extended the linear region to higher conversions, to >90% for the Ni-only catalyst and to ~99% for the $NiZn_2$ one (see inset plot). This effect of CO is similar to that found previously for a Ni/SiO_2 catalyst and can be explained in terms of two effects [10]. Adsorption of CO inhibited the adsorption of H_2, which favoured reaction (1) over (2)

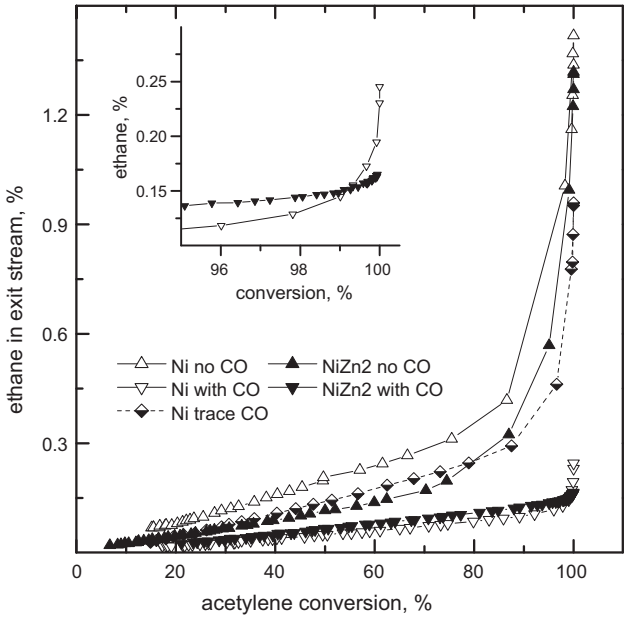

Fig. 4. Ethane production versus acetylene conversion for $Ni/MgAl_2O_4$ and $NiZn_2/MgAl_2O_4$ catalysts under standard conditions with and without 550 ppmv CO present (0.2 g sample, 2% C_2H_2, 20% H_2 in He with total flow rate of 50 cm^3/min).

over the full conversion range, and also inhibited the adsorption of ethylene at high conversions, which disfavoured reaction (3).

It is also apparent from Fig. 3 that the effect of zinc on selectivity is much less than that of CO. In the absence of CO, and in accordance with the findings of Studt et al. [9], the $NiZn_2$ catalyst produced less ethane than did the Ni-only catalyst. However this was not always true when CO was present. The $NiZn_2$ catalyst yielded slightly more ethane at conversions below a cross-over point at ~99.2% conversion (inset plot). The implication was that in the presence of CO, the zinc had a slightly negative effect on the primary selectivity, i.e. it degraded activity for reaction (1) versus (2). A possible explanation is that Zn (or unreduced ZnO) present on the Ni surface impeded the adsorption of acetylene marginally more than that of hydrogen, which is smaller. In this case the ratio of hydrogen atoms to acetylene on the surface would rise which would favour the formation of ethane, which requires the addition of four H atoms in total, over that of ethylene, requiring two. On the other hand, the presence of zinc had significant benefits at very high conversions, presumably through inhibition of reaction (3). The possible explanation here is that Zn or ZnO, like CO, acted through inhibition of ethylene adsorption when the acetylene had largely disappeared.

As expected, the run carried out using the Ni-only catalyst with a trace of CO still present exhibited intermediate behaviour with ethane production above that seen with CO present but significantly below that for the CO-free run.

Table 2
Selectivity at 75% acetylene conversion for $Ni/MgAl_2O_4$ and $NiZn_2/MgAl_2O_4$.

Catalyst	Feed CO (ppmv)	Selectivity (%)					
		C_2H_4	C_2H_6	CH_4	C_3	i-C_4	Other[b]
$Ni/MgAl_2O_4$	0	47	20	0.26	1.5	1.2	30
	550	34	5	0.54	1.6	3.3	56
	Trace	46	14[a]	0.32	1.8	1.3	37
$NiZn_2/MgAl_2O_4$	0	60	12	0.21	1.3	0.5	26
	550	54	6	0.23	1.4	1.9	36

[a] This value increased from 10 to 16% over the linear conversion region as the trace quantity of CO was slowly flushed from the system.
[b] Calculated by carbon mole balance difference. Includes n-C_4, higher gaseous products and carbonaceous material deposited on the catalyst.

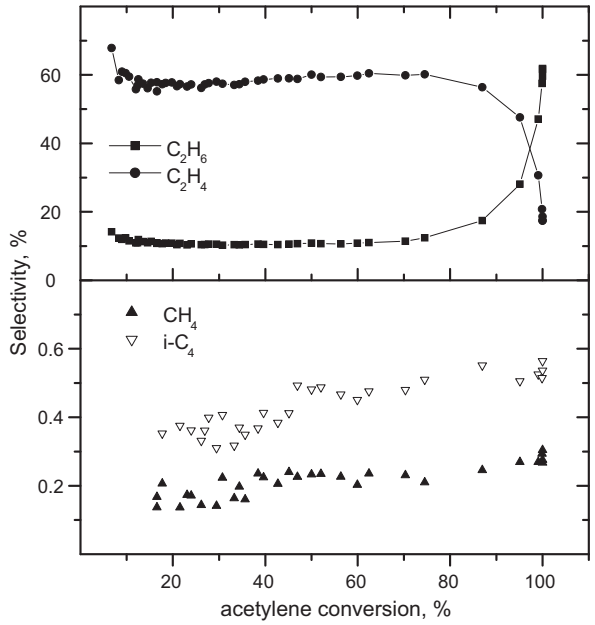

Fig. 5. Selectivity to major and minor products versus acetylene conversion for $NiZn_2/MgAl_2O_4$ with a trace of residual CO present under standard conditions (0.2 g sample, 2% C_2H_2, 20% H_2 in He with total flow rate of 50 cm^3/min).

3.4. Overall production distribution

The selectivities to all the products analysed here as a function of acetylene conversion showed a typical pattern, illustrated in Fig. 5 using data for the $NiZn_2$ catalyst in the absence of CO. Selectivities to both ethane and ethylene were constant to >70% conversion above which the selectivity to ethane increased steeply at the expense of ethylene. On the other hand, production of the minor products, methane and iso-C_4 (isobutene and isobutane) showed a steady increase over the entire conversion range. C_3 products (not shown) also seemed to increase but the scatter in the data made this trend less certain.

The other four systems showed the same general pattern. However selectivities, when interpolated to the same conversion in the linear region, varied widely as shown by the values for 75% conversion in Table 2. Both the Ni-only and $NiZn_2$ exhibited substantially lower selectivity to ethane and, to a lesser extent, ethylene when CO was present. The fall-off was balanced partly by increases in the minor products, CH_4 and i-C_4, but largely by an increase in quantity of n-C_4 and higher products. Although not analysed here, our previous work with Ni/SiO_2 [20,21] found that the gaseous components of the latter were largely even-numbered 1- and 2-alkenes and dienes in amounts that fell with carbon number in the manner of a Fischer–Tropsch distribution with a low α-value.

The effect of CO can be rationalised as follows. Under reaction conditions the nickel surface was largely covered with adsorbed acetylene. Addition of a surface hydrogen atom to the adsorbed acetylene formed a reactive intermediate (half-hydrogenated state), which has two pathways for reaction. Addition of surface hydrogen atom(s) lead to gaseous C_2 products, ethylene through a single addition and ethane through multiple addition. Alternatively the reactive species may undergo oligomerization through addition to adsorbed acetylene. Carbon monoxide competes with gaseous hydrogen for adsorption sites, lowering the number of surface hydrogen atoms. This disfavours hydrogenation to C_2 products and correspondingly favours reaction through oligomerization or other competing processes such as carbon-carbon bond cleavage to form C_1 intermediates from which CH_4 and C_3 compounds are derived. A lower surface hydrogen concentration would also be expected to disfavour the formation of ethane, which requires three hydrogen additions to its half-hydrogenated progenitor, relative to that of ethylene which requires only one, again in agreement with the observed effect of CO.

The data in Table 2 also indicates that the $NiZn_2$ catalyst was somewhat more selective towards C_2 products, ethylene and ethane combined, than the Ni-only one and that the presence of CO lowered the C2 selectivity of the $NiZn_2$ catalyst to a considerably lesser extent. As before, a possible explanation is that Zn (or unreduced ZnO) present on the Ni surface acts to reduce the number of adjacently adsorbed acetylene species and hence the probability of adding adsorbed acetylene to the reactive half-hydrogenated state. Surface hydrogen atoms, being smaller and more mobile would be less impeded by the presence of Zn or ZnO.

4. Conclusions

Both the addition of zinc and the presence of gaseous CO have an inhibitory effect on the rate of hydrogenation of acetylene over nickel. Carbon monoxide also induces a substantial fall in the wastage to ethane for both Ni and $NiZn_2$ systems. Zinc lowers the selectivity to ethane to some extent when CO is absent but this effect is present only at extremely high conversion when CO is present.

Acknowledgments

This work was carried out at a time when one of us (D.L.T.) was a consultant to the CSIRO Earth Science and Resource Engineering and was supported by that organisation. The CO chemisorption measurements were carried out at CSIRO Earth Science and Resource Engineering by Dr. Ken Chiang.

References

[1] L.K. Frevel, L.J. Kressley, United States Patent 2,802,889 (1957).
[2] M.M. Johnson, D.W. Walker, G.P. Nowack, United States Patent 4,404,124 (1983).
[3] E. Sughrue, M. Johnson, R.J. Callejas, in: Proceedings of the 5th Ethylene Producers Conference, vol. 2, Houston, March 1993, AIChE, pp. 448–460.
[4] E.L. Mohundro, in: Proceedings of the 15th Ethylene Producers Conference, New Orleans, March 2003, AIChE, pp. 1038–1067.

[5] A. Borodzinski, G.C. Bond, Catal. Rev. Sci. Eng. 48 (2006) 91–144.
[6] A. Borodzinski, G.C. Bond, Catal. Rev. Sci. Eng. 50 (2008) 379–446.
[7] L.R. French, W.M. Skinner, United States Patent 3,691,248 (1972).
[8] A.B. Stiles, in: B.E. Leach (Ed.), Applied Industrial Catalysis, vol. 2, Academic Press, New York, 1983, pp.131–132.
[9] F. Studt, F. Abild-Pederson, T. Bligaard, R.Z. Sorensen, C.H. Christensen, J.K. Norskov, Science 320 (2008) 1320–1322.
[10] D.L. Trimm, I.O.Y. Liu, N.W. Cant, Appl. Catal. A 374 (2010) 58–64.
[11] K. Breuer, J.H. Teles, D. Demuth, H. Hibst, A. Schafer, S. Brode, H. Domgorgen, Angew. Chem. Int. Ed. 38 (1999) 1401–1405.
[12] D. Trimm, N. Cant, Y. Lei, Catal. Today 145 (2009) 163–168.
[13] P. Nash, Y.Y. Pan, Bull. Alloy Phase Diag. 8 (1987) 422–430.
[14] I. Barin, Thermochemical Data of Pure Substances , VCH, Weinheim, 1989.
[15] X. Gao, J.-Y. Cheng, X.-Y. Fu, H.-M. Wang, J. Nat. Gas. Chem. 4 (1995) 113–118.
[16] J.R.A. Sietsma, J.D. Meeldijk, M. Verluijs-Helder, A. Broersma, A.J. van Dillen, P.E. de Jongh, K.P. de Jong, Chem. Mater. 20 (2008) 2921–2931.
[17] M. Pospisil, V. Cuba, D. Polakova, J. Therm. Anal. Calorim. 75 (2004) 35–50.
[18] N. Iwasa, S. Masuda, N. Ogawa, N. Takezawa, Appl. Catal. A 125 (1995) 145–157.
[19] J.R. Anderson, K.C. Pratt, Introduction to Characterization and Testing of Catalysts , Academic Press, Sydney, 1985, p. 7.
[20] D.L. Trimm, I.O.Y. Liu, N.W. Cant, J. Mol. Catal. A: Chem. 288 (2008) 63–74.
[21] D.L. Trimm, I.O.Y. Liu, N.W. Cant, J. Mol. Catal. A: Chem. 307 (2009) 13–20.